Towards a single-molecule FRET study of Frauenfelder's nonexponential rebinding of CO in myoglobin

Eskandari Alughare, Z.

5

FRET to a distribution of acceptors at the ensemble and single-molecule levels

Theodor Förster some 80 years ago predicted a stretched-exponential fluorescence intensity decay under ensemble conditions. This is related to a distribution of acceptors in the vicinity of each donor; the decay rate depends on the concentration of acceptor around the donor. These non-exponential kinetics arise from a distribution of the exponential steps. In chapter 5, we first tested the consistency of Förster´s theory by studying an ensemble of the acceptors (ATTO575Q) around the donor (Azaoxa-triangulenium, ADOTA) for different concentrations of the acceptor in a thin polymeric layer. The advantage of a dye-doped polymer layer is that it allows for control of the dispersion of the dye molecules in the polymer films and prevents any type of quenching other than that due to FRET. Our single-molecule study showed that histograms of the decay rates of single ADOTA molecules are much more sensitive to the heterogeneity than the average non-exponential decay.

5.1 Introduction

Single-molecule spectroscopy has become an established technique to uncover heterogeneity in soft-matter and biological systems, for example, to study protein folding, [1] nucleic acid dynamics, [2] and to monitor electron transfer events in metalloproteins. [3] Although the interpretation of the complex signals in biological systems is challenging, fluorescence resonance energy transfer (FRET) signals between donor and acceptor at the single-molecule level provide reliable information about the individual single molecules and about their surroundings.
The non-radiative energy transfer called FRET proceeds from a photoexcited donor fluorophore to an acceptor molecule and competes with donor fluorescence for donor-acceptor distances in the 1-10 nm range. The FRET rate depends on the distance between donor and acceptor (r) and is inversely proportional to the sixth power of r (Eq. 1.10). The FRET efficiency (*E*) is defined as the fraction of donor excitations that are transferred to the acceptor. The histogram of FRET efficiencies and the corresponding donor-acceptor distances extracted from single-pair FRET data make it possible to follow the structural dynamics of biomolecules over time and to distinguish the different surrounding environments of single molecules. However, in ensemble experiments, both the spatial and temporal heterogeneities are averaged out, and most of the information about the complexity of system is lost. [4-8]
The aim of this chapter is to reveal the heterogeneity of a FRET process from single donor molecules to a set of acceptor molecules randomly distributed in space around each individual donor. This problem has been treated for an ensemble of donors by Theodor Förster in 1949. [9] He found a strongly non-exponential decay for the average donor fluorescence, which under reasonable assumptions, decays as a stretched exponential, $\exp\left[-\sqrt{\frac{t}{\tau_0}}\right]$. Through single-molecule measurements, we want to show that each single donor molecule decays as a single exponential, and that the stretched-exponential decay arises purely from the spatial averaging over donor molecules, with their individual distributions of acceptor molecules around each of them. For this, we design a system of donors and acceptors with a low concentration of donors and a higher concentration of acceptors, giving rise to a distribution of distances between each donor and a large number of acceptors in its vicinity. We will study FRET at both ensemble and single-molecule levels. We will measure fluorescence decays of the donors and plot histograms of donor lifetimes in presence of acceptors.

5.1.1 Non-fluorescent quenching

As we discussed in chapter 1 (Figure 1.4B), FRET does not require the acceptor to be fluorescent. When the fluorescence of the donor is quenched by the acceptor, the fluorescence intensity and the lifetime of the donor will change. This kind of FRET to a non-fluorescent acceptor has some advantages. For example, since the acceptor itself is not fluorescent, the background and related noise are reduced, which improves the signal-to-noise ratio, particularly for high concentrations of acceptors. Another advantage is the extended observation times because the acceptor dyes do not readily photo-bleach. Moreover, such studies prevent the problem of cross talk in emission detection, when the emission of both donor and acceptor may contribute to the detected signal.

Here, we used a long-lifetime fluorescent dye, ADOTA, as the donor and a non-fluorescent quencher (ATTO575Q) as the acceptor for both ensemble and smFRET studies. Note that the geometry of Fig. 5.1 is not exactly the random 3D distribution postulated by Förster for a homogeneous solution. However, due to the symmetry with respect to the plane interface, the situation in Fig. 5.1 corresponds to a 3D distribution with half the concentration of acceptors.

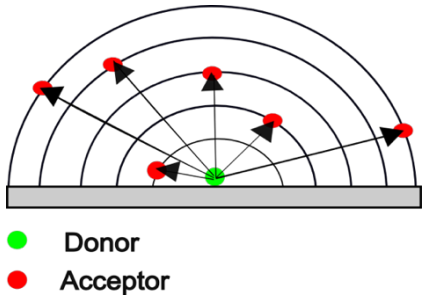

Figure 5.1 *A distribution of acceptors around a donor with different distances. The green dot represents the donor on the surface and the red dots are the acceptors distributed at various distances around the donor.*

5.1.2 Donor: Long-lifetime fluorescent ADOTA dye, a triangulenium dye

The azaoxa-triangulenium fluorophores are organic molecules with planar and rigid structures in which three aromatic rings are bonded to a central carbon atom with a positive charge. This kind of red fluorophores is known as the longest-lived red emitting organic fluorophores because their lifetime in both protic and aprotic solvents is around 20-50 ns. Azadioxa-triangulenium (ADOTA) dyes absorb and emit in the red with a high quantum yield, long fluorescence lifetimes (16-20 ns) and high fluorescence anisotropy, close to the theoretical limit, 0.4. [10-12] These special characteristics of ADOTA make them suitable probes for fluorescent lifetime imaging (FLIM), time-gated fluorescence imaging, fluorescence lifetime and polarization measurements. [13,14]

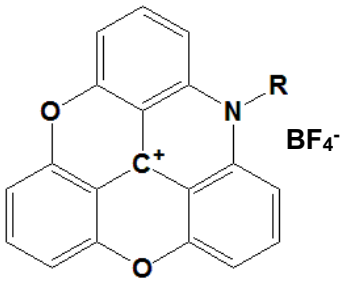

4BF$_4$.ADOTA

Figure 5.2 *The chemical structure of azadioxa-triangulenium dye (ADOTA)* [10,11]

5.1.3 Acceptor: ATTO575Q, a non-fluorescent quencher dye

Here, we used the ATTO 575Q as a novel fluorescence quencher. This dye has an absorption spectrum with maximum absorbance at 582 nm (Figure 5.3) with a molar extinction coefficient of 1.2 x 10^5 M^{-1} cm^{-1}, and high thermal and photo-stability. ATTO 575Q is a cationic dye. [15]

5.1.4 Calculation of the Förster radius R_0 for ADOTA (donor)- ATTO575Q (acceptor)

As we showed in chapter 1 (eq. 1.8), the Förster radius R_0 (the distance at which the energy transfer efficiency is 50%) depends on the overlap of the donor emission spectrum with the acceptor absorption spectrum and on their mutual molecular orientation. The calculated R_0 assuming isotropic dye orientations is 6.38 nm. Figure 5.3 shows the absorption spectrum of ATTO575Q as the acceptor and the emission spectrum of ADOTA as the donor. Figure 5.4 shows that these spectra overlap strongly, leading to a large FRET radius.

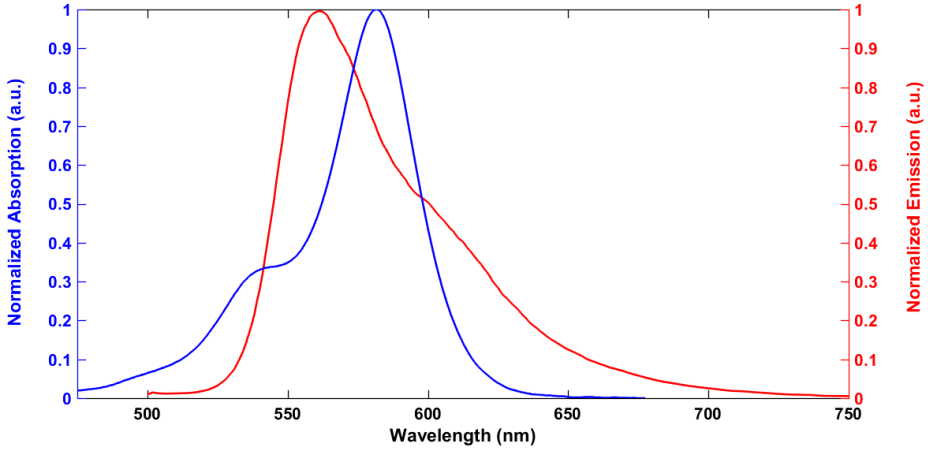

Figure 5.3 *The normalized absorption spectrum of ATTO575Q as acceptor (blue, left axis), [15] and the normalized fluorescence spectrum of ADOTA as donor (red, right axis) in phosphate buffer, pH=7, at room temperature.*

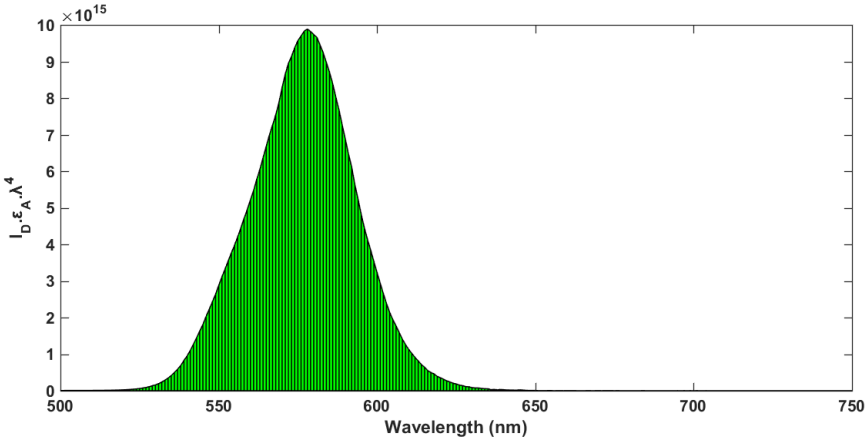

Figure 5.4. *Product of the normalized absorption spectrum of the ATTO 575Q as the acceptor and of the normalized fluorescence spectrum of the ADOTA as the fluorescence donor. The overlap integral is proportional to the area under this curve (green area), based on equation 1.8 (as* $\int \bar{F}_D(\lambda)\epsilon_A(\lambda)\,\lambda^4 d\lambda$*).*

5.1.5 Ensemble fluorescent quenching

To study the fluorescent characteristics of a donor in presence of acceptors, it is crucial to avoid any chemical quenching due to aggregation. The concentrations have been chosen low enough that the dyes are well soluble in the different polymers used. Moreover, the solid polymers immobilize the donor and acceptor molecules and prevent rotational and translation diffusion. Lifetime measurements will be performed

on times short enough that donor and acceptor molecules will remain at fixed positions during the acquisition of the data. [14,16,17]

5.1.6 Ensemble measurements of fluorescence quenching in solid-state dye-doped polymer layers

To avoid the possibility of specific interactions between donor and acceptor in a 3D solution, we decided to incorporate the two dyes into different, immiscible polymers, PMMA and PVA. The donor dye (ADOTA) was doped into a poly(methyl methacrylate) (PMMA) polymer layer, which was spin-coated on the glass surface. The film thickness changes as a function of spin-coating conditions such as the weight percentage of the polymer in the solution, the rotation speed of the spin coater, etc. The uppermost layer of poly(vinyl alcohol) (PVA) was doped with the acceptor dye ATTO575Q and deposited homogeneously (drop casting) on top of the PMMA (Figure 5.5).
We optimized the spin-coating conditions to obtain a thin but regular ADOTA-doped PMMA layer of 6 nm thickness, whereas the acceptor-doped PVA layer was much thicker, about 100 nm. The finite thickness of the PMMA layer introduces a deviation from the Förster model, as the minimum distance between donor and acceptor will be 3 nm on average. We assume this deviation is not too large and does not significantly affect our results.

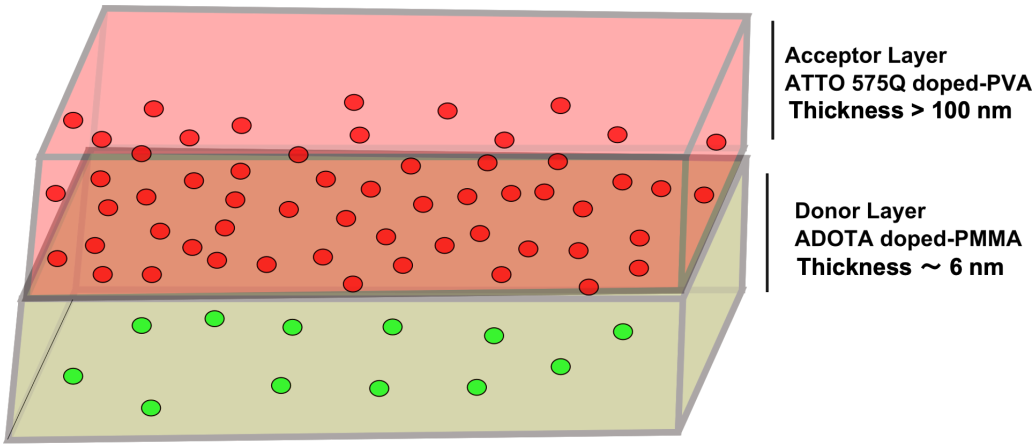

Figure 5.5 *Ensemble sample consisting of two layers. Top layer: ATTO575Q (acceptor) dopped-PVA, thickness 100 nm. Bottom layer: ADOTA (donor)-doped PMMA, thickness 6 nm. The layers were deposited on a glass coverslip.*

5.1.7 Fluorescence quenching as a function of quencher concentration

Due to the distribution of acceptors around each donor molecule, the fluorescence decay of an ensemble of donors is strongly non-exponential. Förster [9] derived an expression for the average fluorescence decay of an ensemble of donor dyes interacting with a random spatial distribution of acceptors, assuming that the distance between the donors was very large compared to the Förster radius. This decay takes the following simple form:

$$\overline{Q(t)} = e^{\frac{-t}{\tau_0} - \frac{N{R_0}^3\sqrt{\pi}}{{R_g}^3}\sqrt{\frac{t}{\tau_0}}} \quad 5.1$$

where t, τ_0 are time and the fluorescence lifetime of the free donor dye, respectively, and R_0, R_g, N are the Förster radius, the radius of a large spherical volume of the acceptor solution, and the number of acceptor molecules in this spherical volume. We can reformulate Eq. 5.1 by using the concentration *C* of the acceptor:

$$\overline{Q(t)} = e^{\left[\frac{-t}{\tau_0} - \frac{4\pi C\ N_A{R_0}^3\sqrt{\pi}}{3}\sqrt{\frac{t}{\tau_0}}\right]} \quad 5.2$$

where N_A is the Avogadro number (6.023 x 10^{23} molecule/mole).
Here, our aim is to study an ensemble and measure the averaged decay of the donor dyes and how it varies with the acceptor concentration.

5.1.8 Single-molecule fluorescence quenching

The measurement of the fluorescence of an ensemble provides average values of the fluorescence characteristics such as lifetime and fluorescence intensity. Single-molecule observations, however, will eliminate ensemble averaging and will reveal the hidden heterogeneity of the sample. [14]
To study fluorescence quenching of a single donor molecule in presence of a distribution of acceptors, we used the same geometry and polymers as in the ensemble experiment (as described in section 5.1.5), but with an even lower concentration of donors.
Our first control experiment was to study the fluorescence decay of a single ADOTA molecule in PMMA in the absence of any acceptor (ATTO575Q) (Figure 5.5A). In this case we spread an acceptor-free PVA layer on top of the ADOTA-doped PMMA, to compare both with the ensemble results (see section 5.1.5) and with the single-molecule results (see section 5.2.7).
The second control experiment measured of the fluorescence quenching of single ADOTA molecules (donor) in the presence of ATTO575Q acceptors dispersed in the PMMA polymer matrix as well as in the PVA top layer with the same concentration of acceptors in both layers. The aim of this control experiment is to rule out sticking of donors and/or acceptors at the interface between the two polymers. For example, in the ADOTA-doped PMMA bottom layer and ATTO 575Q-doped PVA top layer, there is the possibility of the dyes sticking to the interface. Sticking to the glass-PMMA interface or to the PMMA-air interface would make for a very inhomogeneous distribution of donor-acceptor pairs.
The PMMA polymer layer was spin-coated on the glass surface and the concentration of ADOTA was around 1000 times less than in the ensemble sample, in order to reach the single-donor regime. The spin-coating procedure was the same for all samples. The thickness of donor-doped PMMA layer was measured to be 6 nm on average, whereas the thickness of the acceptor-doped PVA layer was more than 100 nm.

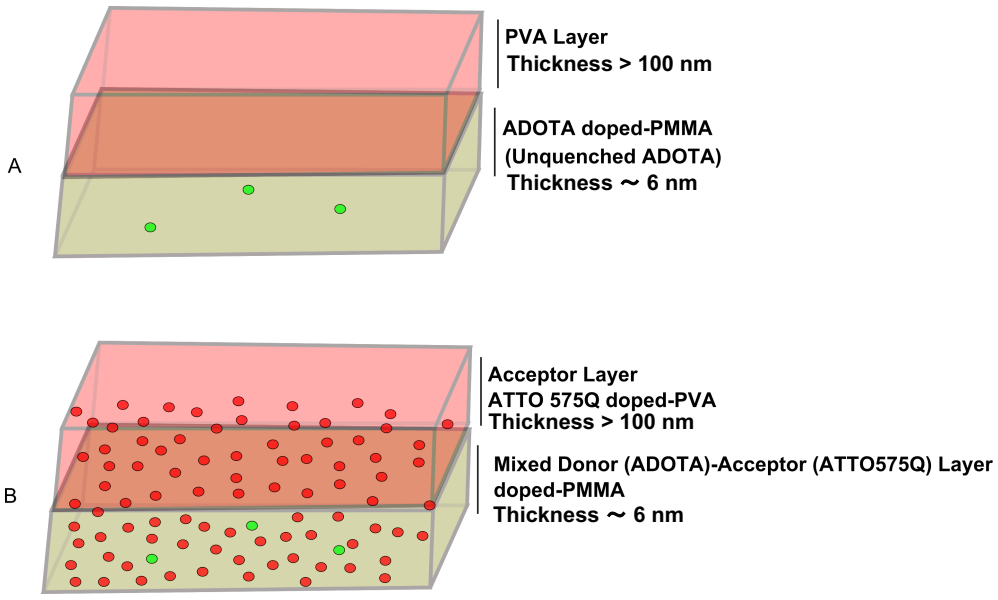

Figure 5.6 *Solid-state dye-doped polymer in the single-molecule fluorescence quenching assay. (A) ADOTA single molecule doped PMMA in the absence of acceptor (B) Both ADOTA (donor) and ATTO575Q (acceptor) dyes dispersed in PMMA polymeric matrix while the PVA top layer also contains the acceptor.*

5.2 Results

5.2.1 Confocal setup

The confocal setup was a home-built microscope in which ADOTA dye (donor) is excited with a pulsed laser at 485 nm with a pulse rate of 26 MHz. The schematic illustration of the setup is shown in Figure 5.7. The collected photons were detected with time-correlated single-photon counting (TCSPC) and converted by the SymphoTime software to fluorescence decays.

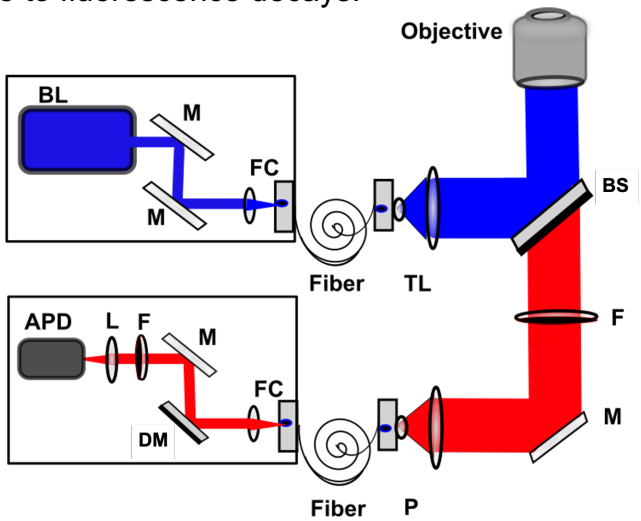

Figure 5.7 *Scheme of our home-built confocal setup for fluorescence decay measurements of FRET from a ADOTA donor to ATTO575Q acceptors. BL=Blue Laser, M=Mirror, FC= Fiber Collimator, L=Lens, TL=Telescope (Beam Expander), BS=Beam splitter, F=Filter, P=Pinhole, DM=Dichroic Mirror, APD=Avalanche Photodiode Detector.*

5.2.2 Surface preparation of glass microscope cover slips

The surface preparation of clean glass microscope coverslips (No. 1, = 25 mm Hecht-Assistent, Sondheim, Germany) was done according to the following protocol:
Both sides of the coverslip glasses were first washed with acetone, then blown dry with nitrogen gas. Then, both sides of the coverslips were rinsed with isopropanol and blown dry with nitrogen. The remaining solvents on the surface of the coverslips were removed through heating the coverslips for 2.5 hours at 170°C.

5.2.3 Ensemble sample preparation

The thin film of ADOTA-doped PMMA was prepared by spin-coating dilute ADOTA dye solutions (200 nM) in chloroform containing 1.0% w/w PMMA (average Mw 120000, Sigma Aldrich) onto the surfaced-prepared coverslips. The spin-coating program consists of sequential steps including: 10 seconds (500 rpm), 60 seconds (2000 rpm), and 10 seconds (4000 rpm). The samples were dried in the dark at room temperature. The fluorescent dye, Biotinylated-ADOTA, was purchased from the KU dye company, Copenhagen, Denmark. There were other possibilities of functional groups linked to the ADOTA such as amine, carboxyl, or amide groups instead of the biotin functional group but we selected the Biotinylated-ADOTA to decrease the possibility of chemical interaction of ADOTA to the surface of glass via this group. The thickness of the samples was measured with an AFM thickness profiler (BRUKER, Germany). Figure 5.8 shows the thickness profile of a prepared sample. The sample with 0.1% w/w PMMA has an average thickness of 6 nm (Figure 5.8A-B)

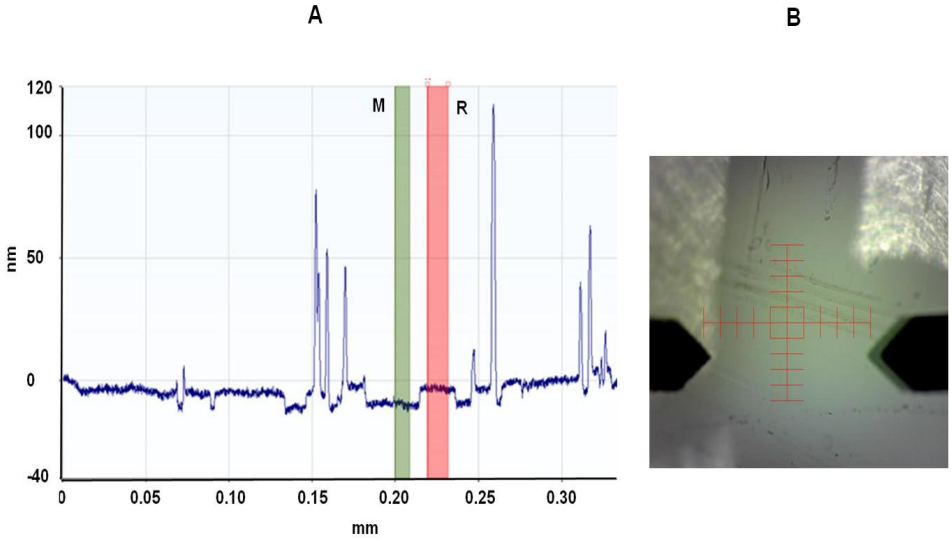

Figure 5.8 *The thickness profile of the prepared sample of ADOTA-doped PMMA spin-coated on the glass coverslip, and measured by an AFM thickness profiler. (A-B) Measurement of the thickness of the thin polymeric monolayer (with an average thickness of 6 nm). The sharp structures are caused by impurities on the surface. Scratching with the tip of the AFM makes a depression in the surface, the depth of which corresponds to the film thickness. The sample was prepared with 0.1% w/w PMMA.*

The acceptor (ATTO575Q)-doped PVA layers were prepared by diluting a few drops of an aqueous solution containing ATTO575Q mixed with 1% w/w PVA (99+% hydrolyzed, average Mw 120,000, Sigma Aldrich) in water to reach the desired final

concentration in PVA (400 μM, 1 mM, 3 mM, and 5 mM) and was spread on top of the ADOTA-doped PMMA layer on the glass surface. The sample was dried at room temperature over time in the dark. The non-fluorescent dye, ATTO575Q was purchased from Atto-Tec (Siegen, Germany).
It should be noted that the spin-coating rate and the polymer weight percentage are crucial to make a very thin polymeric layer. For all samples in this chapter, this protocol was applied to have a very thin layer. The reason of preparation of such a thin polymeric layer is that the distance between the donor and acceptor should be between 1-10 nm to be able to study FRET due to the quenching of the donor in presence of acceptors.

5.2.4 Ensemble fluorescent lifetime quenching measurements

The fluorescence time traces and fluorescence decay curves of ADOTA-doped PMMA (bottom layer) in presence of ATTO 575Q-doped PVA (with the different concentrations 400 μM, 1mM, 3mM, and 5mM) were recorded using our confocal microscope. Based on equation 5.2, the fluorescent decay of ADOTA (donor) is substantially quenched when the concentration of quencher (ATTO 575Q) in the top polymer layer is increased. Figure 5.9 shows the experimental fluorescence decays (dark colors) and the fit to equation 5.2 (light colors). The theoretical fits in this figure were obtained by varying the concentration and the concentrations are 0.25, 1.1, 2.8, and 5.7 mM for the experimental used concentration of 0.400 mM, 1 mM, 3 mM, and 5 mM respectively. It should be moted that the fits have been convoluted with IRF to be compatible with experimental data.

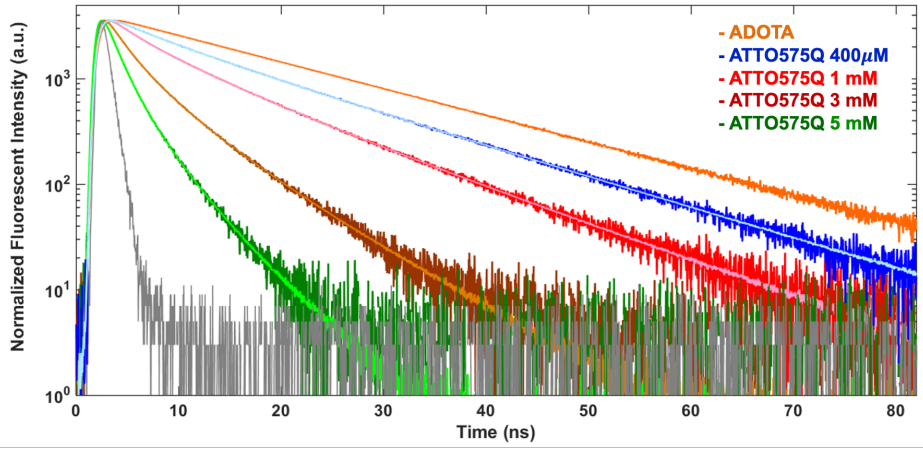

Figure 5.9 *Fluorescence decay (dark colors) and fit (lighter colors) for ADOTA donors in presence of four different concentrations of ATTO575Q acceptors: 400 µM (blue), 1 mM (red), 3 mM (brown), 5 mM (green). The orange-colored decay is the mono-exponential decay of ADOTA in the absence of quencher. The gray decay curve is the Instrument Response Function (IRF). The fits in this figure were obtained by varying the concentration (adjustable parameter) and the best fits yielded with concentrations of 0.250, 1.1, 3.2, and 5.7 mM corresponding with the traces obtained with concentrations of 0.400 mM, 1 mM, 3 mM, and 5 mM respectively.*

5.2.5 Single-molecule sample preparation

To study the donor (ADOTA) fluorescence in the presence of acceptors (ATTO575Q) at the single-molecule level, we decreased the donor concentration to 200 picomolar.

All the steps for the surface preparation of coverslip glasses and dye-doped polymer layers are the same as for the ensembles described above, except for the lower concentration of ADOTA.

5.2.6 Single-molecule fluorescence lifetime measurements

The sample to study the single-molecule quenching was prepared as described in 5.2.3, and 5.2.5. The single-molecule images, fluorescence time traces and fluorescence decay curves were recorded using a confocal microscope. The scan image size is 10 µm × 10 µm. The surface scans were measured with the confocal microscope and the individual lifetimes of single molecules were obtained. Figure 5.10 shows the 10 µm × 10 µm image of a sample of ADOTA-doped PMMA in the absence of quenchers. Each single-molecule time trace of unquenched ADOTA molecules could be collected and showed single-step bleaching with a maximum duration of 2.7 s. All traces gave rise to mono-exponential fluorescence decays with an average lifetime of 18.3 ns and a very limited spread of lifetimes, from 17 to 19 ns.

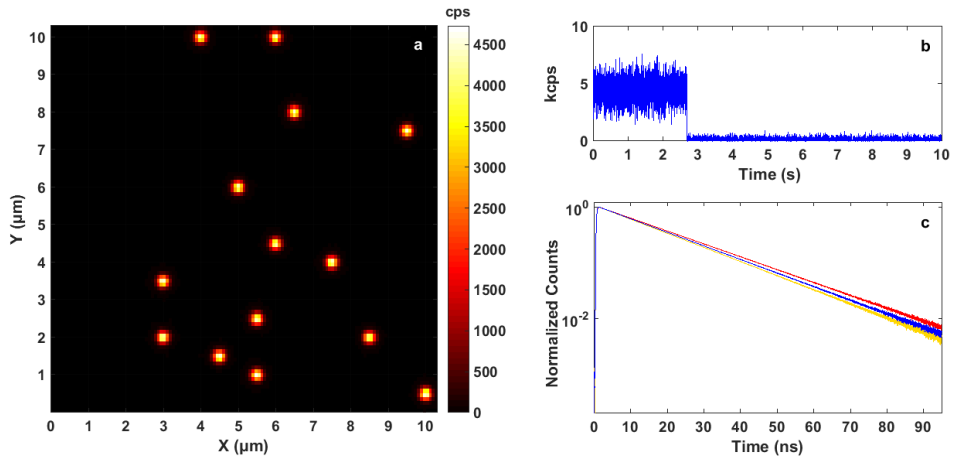

Figure 5.10 Single molecules of unquenched ADOTA: *a) Single-molecule fluorescence image of PMMA doped with ADOTA; b) Single-molecule time trace of ADOTA showing single-step photobleaching after 2.7 s. This time trace was recorded by focusing on a single molecule embedded in the PMMA film for 1 minute; c) Normalized fluorescence decay curves of three single ADOTA molecules showing mono-exponential behavior.*

Figure 5.11 shows a 10 µm × 10 µm image of a sample in which the first PMMA layer, 6 nm thick, was doped with a mixture of ADOTA (donor) and ATTO575Q (acceptors) (1mM). After this first layer was spin-coated on a coverslip, a thick PVA layer (thickness > 100 nm) doped with ATTO 575Q was added. This control experiment is meant to check that there was no sticking of the donor or acceptors to the glass-PMMA interface or to the PMMA-PVA interface. If such sticking occurs, we expect stronger quenching when the acceptors are present in the PMMA layer. In the case of donor sticking to the glass surface, we expect a larger distance on average between the donor and the acceptors, and therefore less quenching on average. We found no significant difference between the measured samples and the controls, which points to the absence of significant sticking of the donor to the glass or of the acceptor to the PMMA. Figure 5.11b shows a single-molecule time trace of a quenched ADOTA showing photoblinking and single-step photobleaching. The fluorescence decay

curves of different single ADOTA molecules in Fig. 5.11c show mono-exponential decays with a wide range of lifetimes. Single-exponential fits are represented as solid lines and fit the decays perfectly.

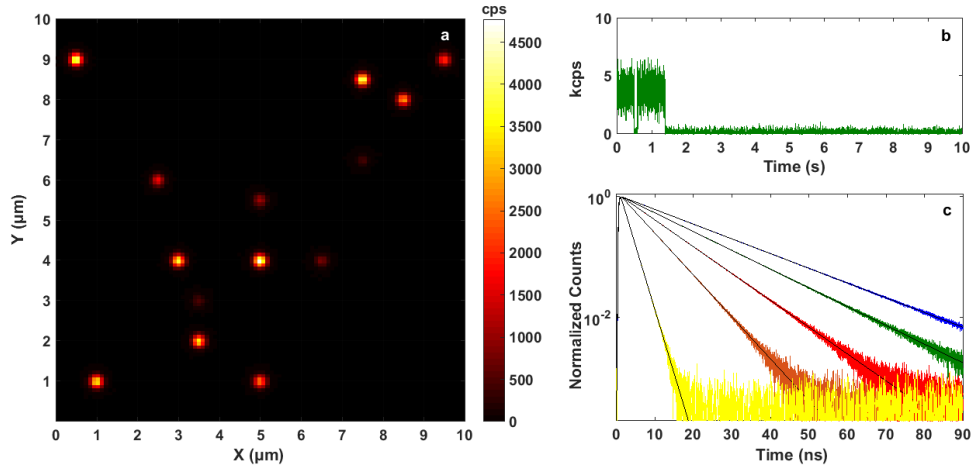

Figure 5.11 Single molecule of quenched ADOTA with ATTO 575Q : *a) A 10 µm × 10 µm image of Single ADOTA molecules doped in PMMA with a mixture of ATTO 575Q (1mM), spin coated on a coverslip glass as a first layer and covered with a thick PVA film doped with ATTO 575Q (1 mM); b) A single-molecule time trace of a partially quenched ADOTA molecule showing photoblinking and single-step photobleaching; c) Normalized fluorescence decay curves of different single ADOTA molecules showing single-exponential decays with a wide range of lifetimes and their mono-exponential decay fits (black lines). Decay curves were recorded by focusing on individual molecules embedded in the PMMA film.*

5.3 Discussion

5.3.1 Comparison of single-molecule results with and without quenchers

In the presence of acceptors (ATTO575Q), the histogram of lifetimes of the ADOTA donor molecules was profoundly altered in comparison to the unquenched histogram (see decays in Fig. 5.10). The lifetime histogram of quenched ADOTA donors show dramatic broadening and heterogeneity, as shown by the yellow plot in Fig. 5.12b, in comparison with the very narrow and homogeneous histogram of unquenched ADOTA in Fig. 5.12a.

To understand better this heterogeneity, we simulated a lifetime histogram of ADOTA donor in the presence of a random 3D distribution of quenchers (ATTO575Q) (see Eqs. 5.2, and 1.11) in which the value of R_0 (Förster Radius), τ_0 (Lifetime of free ADOTA in the absence of acceptor), and C (concentration of ATTO575Q) have been assigned as 6.38 nm, 18.5 ns, and 1 mM. In this simulation, we placed the donor at the origin and distributed acceptors randomly in space around it, with a probability defined by the concentration. Then the total transfer rate towards the acceptors was calculated. As can been seen in Figure 5.12b, both experimental and simulated data show a broad and inhomogeneous distribution of lifetimes, with a significant weight for short lifetimes. Because the time resolution of our time-correlated photon counting apparatus is limited, and because of the weakness of the signals, we cannot measure lifetimes shorter than 0.5 ns. This may explain the large deviation of experimental data from the simulated histogram at lifetimes below 1-2 ns (see Fig. 5.12b).

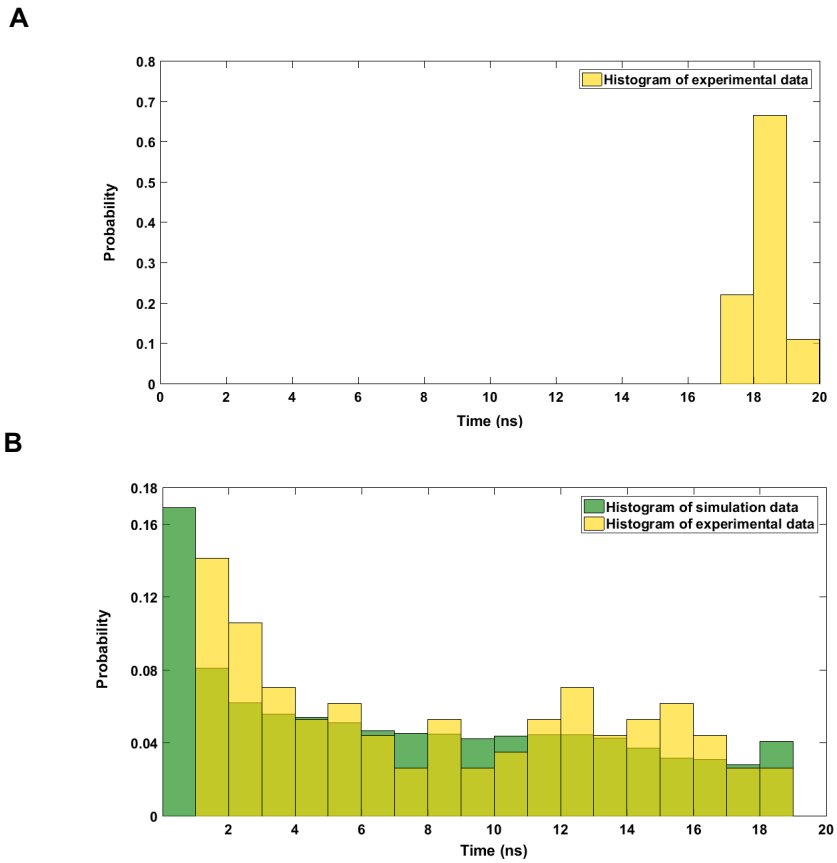

Figure 5.12 *Comparison of data lifetimes histograms of all single molecules from (A) 9 unquenched ADOTA molecules, which shows a low spread of lifetime weighted to long life times and (B) 103 quenched ADOTA molecules in the presence of ATTO 575Q (1mM) (yellow). Simulated data (green) which shows a broad and inhomogeneous distribution of lifetimes and weighted to the short lifetimes, similar to what observed for the experimental data.*

5.3.2 Comparison of ensemble and single molecule results

The single-molecule images and lifetime histograms demonstrate the distribution of individual molecular properties such as intensity and decay rate. These properties are averaged out in the ensemble measurements giving rise to a multi-exponential decay of the donor fluorescence in presence of acceptors. The non-exponential decay is well reproduced by the formula of Förster, as shown in Fig. 5.9. The complex multiexponential decay of the ensemble measurement resolves into a collection of single-exponential decays with very different decay rates for each individual molecule, corresponding to the particular distribution of acceptors that each single donor molecule experiences.

5.4 Conclusion

Some 80 years ago, Theodor Förster predicted a stretched-exponential decay for an ensemble of donors when each of them can transfer energy to a distribution of acceptors. When donor and acceptors are immobilized, this non-exponential kinetics arises from a static distribution of individual exponential decays. In this chapter, we designed ensemble experiments to study transfer from ADOTA donors (Azaoxa-triangulenium) towards a distribution of acceptors (ATTO575Q as quenchers). The

donor was chosen because of its high quantum yield and long fluorescent lifetime. The dyes were placed in thin polymeric layers to immobilize them and to prevent direct chemical interactions between them. The “ensemble” fluorescence quenching data of ADOTA (donor) in presence of ATTO 575Q (acceptor) in Fig. 5.9 fit Förster’s theory (eq. 5.2) very well. As expected, the quenching of the donor increases with the concentration of acceptors.
To compare ensemble results with single donor molecule experiments, we used the same system of donor-acceptor, and varied the acceptor concentration. As expected, the fluorescence decays of single donor molecules were all single-exponential with a wide spread of decay times (see Figure 5.11), as expected for Förster energy transfer towards a fixed distribution of acceptors. The wide distribution of decay rates results into the strongly non-exponential decays of Figure 5.9. On the basis of the lifetime histograms presented in Figure 5.12, we find a remarkable agreement between the observed lifetimes of individual donors and simulations assuming a homogeneous distribution of acceptors in the vicinity of the donors.
In conclusion, the spatial heterogeneity in the ensemble measurements is revealed by single-molecule measurements and show a large spread of local quenching situations. By measuring a large number of single molecules (here 103), we obtain a histogram of exponential lifetimes, which not only reproduce the ensemble results, but give a much more detailed view of the distribution of distances at the level of single molecules, in qualitative agreement with simulations.

References

(1) Deniz, A. A.; Laurence, T. A.; Beligere, G. S.; Dahan, M.; Martin, A. B.; Chemla, D. S.; Dawson, P. E.; Schultz, P. G.; Weiss, S. Single-Molecule Protein Folding: Diffusion Fluorescence Resonance Energy Transfer Studies of the Denaturation of Chymotrypsin Inhibitor 2. *Proc. Natl. Acad. Sci. U. S. A.* **2000**, *97* (10), 5179–5184.

(2) Karymov, M. A.; Chinnaraj, M.; Bogdanov, A.; Srinivasan, A. R.; Zheng, G.; Olson, W. K.; Lyubchenko, Y. L. Structure, Dynamics, and Branch Migration of a DNA Holliday Junction: A Single-Molecule Fluorescence and Modeling Study. *Biophys. J.* **2008**, *95* (9), 4372–4383.

(3) Tabares, L. C.; Gupta, A.; Aartsma, T. J.; Canters, G. W. Tracking Electrons in Biological Macromolecules: From Ensemble to Single Molecule. *Mol. Basel Switz.* **2014**, *19* (8), 11660–11678.

(4) Pradhan, B.; Engelhard, C.; Van Mulken, S.; Miao, X.; Canters, G. W.; Orrit, M. Single Electron Transfer Events and Dynamical Heterogeneity in the Small Protein Azurin from Pseudomonas Aeruginosa. *Chem. Sci. 11* (3), 763–771.

(5) Tabares, L. C.; Kostrz, D.; Elmalk, A.; Andreoni, A.; Dennison, C.; Aartsma, T. J.; Canters, G. W. Fluorescence Lifetime Analysis of Nitrite Reductase from Alcaligenes Xylosoxidans at the Single-Molecule Level Reveals the Enzyme Mechanism. *Chem. Weinh. Bergstr. Ger.* **2011**, *17* (43), 12015–12019.

(6) Zondervan, R.; Kulzer, F.; Kol'chenk, M. A.; Orrit, M. Photobleaching of Rhodamine 6G in Poly(Vinyl Alcohol) at the Ensemble and Single-Molecule Levels. *J. Phys. Chem. A* **2004**, *108* (10), 1657–1665.

(7) Vogel, S. S.; Nguyen, T. A.; van der Meer, B. W.; Blank, P. S. The Impact of Heterogeneity and Dark Acceptor States on FRET: Implications for Using Fluorescent Protein Donors and Acceptors. *PloS One* **2012**, *7* (11), e49593.

(8) Sanabria, H.; Rodnin, D.; Hemmen, K.; Peulen, T.-O.; Felekyan, S.; Fleissner, M. R.; Dimura, M.; Koberling, F.; Kühnemuth, R.; Hubbell, W.; Gohlke, H.; Seidel, C. A. M. Resolving Dynamics and Function of Transient States in Single Enzyme Molecules. *Nat. Commun.* **2020**, *11* (1), 1231.

(9) Förster, V. T. Experimentelle und theoretische untersuchung des zwischenmolekularen übergangs von elektronenanregungsenergie. *Z.Naturforschg*. **1949**, *4a*, 321-327.

(10) Bora, I.; A. Bogh, S.; Rosenberg, M.; Santella, M.; Just Sørensen, T.; W. Laursen, B. Diazaoxatriangulenium: Synthesis of Reactive Derivatives and Conjugation to Bovine Serum Albumin. *Org. Biomol. Chem.* **2016**, *14* (3), 1091–1101.

(11) Robust Long Fluorescence Lifetime Dyes. *KU dyes*.

(12) Sørensen, T. J.; Thyrhaug, E.; Szabelski, M.; Luchowski, R.; Gryczynski, I.; Gryczynski, Z.; Laursen, B. W. Azadioxatriangulenium (ADOTA+): A Long Fluorescence Lifetime Fluorophore for Large Biomolecule Binding Assay. *Methods Appl. Fluoresc.* **2013**, *1* (2), 25001.

(13) Maliwal, B. P.; Fudala, R.; Raut, S.; Kokate, R.; Sørensen, T. J.; Laursen, B. W.; Gryczynski, Z.; Gryczynski, I. Long-Lived Bright Red Emitting Azaoxa-Triangulenium Fluorophores. *PLoS ONE* **2013**, *8* (5), e63043.

(14) Kacenauskaite, L.; Bisballe, N.; Mucci, R.; Santella, M.; Pullerits, T.; Chen, J.; Vosch, T.; Laursen, B. W. Rational Design of Bright Long Fluorescence Lifetime Dyad Fluorophores for Single Molecule Imaging and Detection. *J. Am. Chem. Soc.* **2021**, *143* (3), 1377–1385.

(15) ATTO-TEC GmbH - ATTO-TEC GmbH https://www.atto-tec.com/?language=de (accessed 2022 -04 -29).

(16) Shundo, A.; Okada, Y.; Ito, F.; Tanaka, K. Fluorescence Behavior of Dyes in Thin Films of Various Polymers. *Macromolecules* **2012**, *45* (1), 329–335.

(17) Gushiken, N. K.; Paganoto, G. T.; Temperini, M. L. A.; Teixeira, F. S.; Salvadori, M. C. Substrate for Surface-Enhanced Raman Spectroscopy Formed by Gold Nanoparticles Buried in Poly(Methyl Methacrylate). *ACS Omega* **2020**, *5* (18), 10366–10373.